CHEMISTRY OF MATERIALS

pubs.acs.org/cm

Article

Catalytic Degradation of an Organophosphorus Agent at Zn−OH Sites in a Metal−Organic Framework

Mohammad Rasel Mian, Timur Islamoglu,* Unjila Afrin, Subhadip Goswami, Ran Cao, Kent O. Kirlikovali, Morgan G. Hall, Gregory W. Peterson, and Omar K. Farha*

Cite This: https://dx.doi.org/10.1021/acs.chemmater.0c02373

Read Online

ACCESS | Metrics & More | Article Recommendations | Supporting Information

ABSTRACT: Chemical warfare agents (CWAs), and in particular organophosphorus nerve agents, still pose a significant threat to society due to their continued use despite international bans. While nature has constructed a variety of enzymes that are capable of rapidly hydrolyzing organophosphorus substrates, the poor stability of enzymes outside of buffered solutions has limited their use in practical applications, such as in filters or on protective suits. As a result, we have explored the use of metal−organic frameworks (MOFs) as robust and tunable catalytic materials in which the nodes can be tailored to resemble the active sites found in these enzymes. We identified the Zn-based MOF, MFU-4l, as a promising hydrolysis catalyst due to the presence of Zn(II)−OH groups on the nodes, which are structurally reminiscent of the active sites in carbonic anhydrase (CA), a Zn-based enzyme that has been shown to efficiently catalyze the hydrolysis of phosphate esters. Indeed, MFU-4l can rapidly hydrolyze both the organophosphorus nerve agent, GD, and its simulant, DMNP, with half-lives as low as <1 min, which is competitive with the some of best heterogeneous hydrolysis catalysts reported to date.

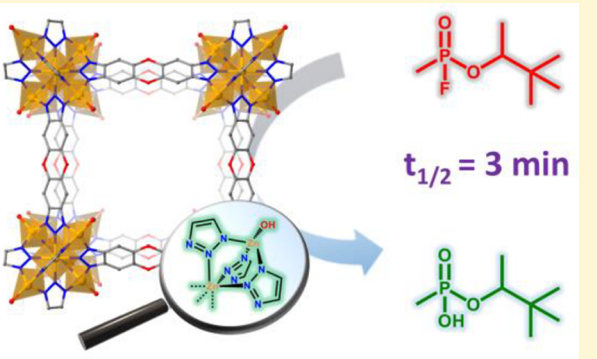

INTRODUCTION

While the Chemical Weapons Convention has banned the use of chemical warfare agents (CWAs), or chemicals intended to harm exposed people through alterations in physiological functions, the use of CWAs has remained prevalent in recent years.[1−3] In particular, organophosphorus nerve agents comprise a class of CWAs that are some of the most toxic chemicals known to humanity, and their continued worldwide use despite international prohibition has warranted the development of materials capable of rapidly detoxifying these nerve agents.[4] Nature has elegantly produced a variety of enzymes that can effectively hydrolyze organophosphorus substrates, and while their structures differ greatly, these enzymes all feature Lewis acidic metal−oxy/hydroxy species that function as active sites for catalysis.[5−8] For example, the enzyme phosphotriesterase (PTE) contains an active site in which two Zn(II) ions are bridged by a hydroxyl anion, enabling PTE to rapidly hydrolyze organophosphorus nerve agents, such as sarin, cyclosarin, and soman.[9−11] Although these enzymes exhibit great performance for the catalytic hydrolysis of nerve agents, the poor stability of enzymes outside of buffered solutions and after long-term storage has precluded their use in practical applications, such as coatings on protective suits or on filters used in masks.

Drawing inspiration from biology, researchers sought to develop robust metal oxide-based materials that could sufficiently mimic the active sites in enzymes while also exhibiting greater stability than enzymes in a wider range of conditions. In particular, metal−organic frameworks (MOFs) have been recognized as a versatile platform for the design of atomically precise heterogeneous catalysts that are capable of meeting these stringent requirements.[12−18] MOFs are two- or three-dimensional crystalline porous frameworks built from metal-based nodes and multitopic organic linkers, and tuning the composition of these components enables precise control over the properties of these materials, resulting in MOFs that offer promising solutions to a variety of global challenges, including catalysis, gas storage and separation, water purification, drug delivery, and sensing, among others.[13,19−26] Specifically, MOFs featuring a Zr_6-based node (Zr-MOFs) have exhibited remarkable catalytic activity toward the hydrolysis of nerve agents and nerve agent simulants, which are molecules with similar functionality but lower toxicity, in basic aqueous solutions.[27−30] The Zr_6 nodes in Zr-MOFs feature bridging Zr−OH−Zr moieties that are similar to the

Received: June 6, 2020
Revised: July 20, 2020

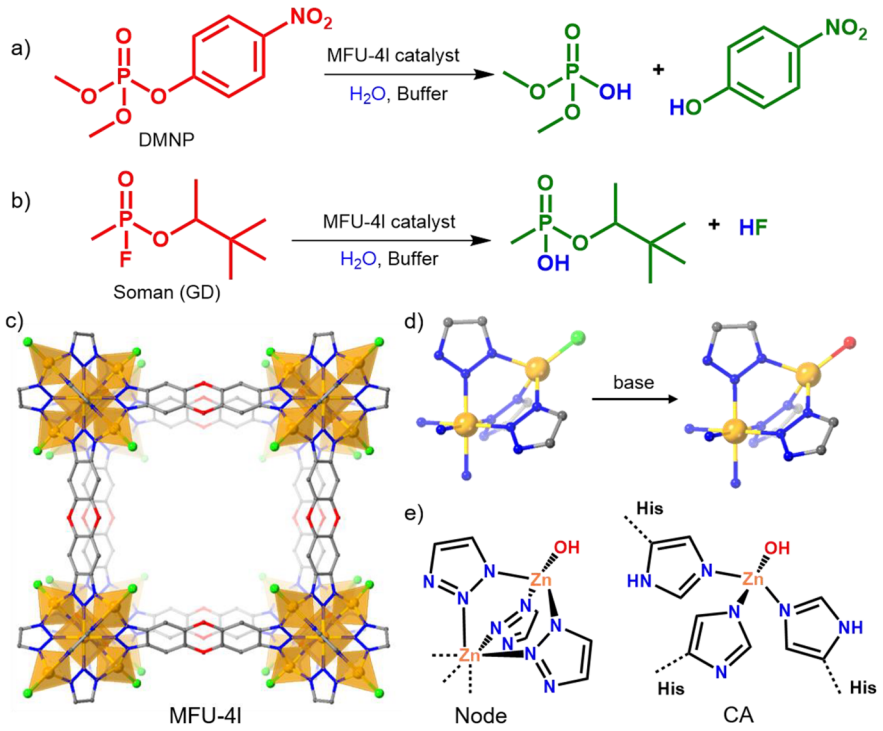

Figure 1. Hydrolysis reaction of (a) the phosphonate-based nerve agent simulant DMNP (dimethyl (4-nitrophenyl) phosphonate) and (b) the real nerve agent GD (*O*-pinacolyl methylphosphonofluoridate). (c) Structural representation of MFU-4l. (d) Cl^- ion is replaced with OH^- after base treatment. (e) Comparison between the active site in MFU-4l and carbonic anhydrase (CA). Brown, Zn; green, Cl, gray, C; blue, N; and red, O. Hydrogen atoms are omitted for clarity.

Lewis acidic active sites found in enzymes such as PTE, and strong Zr(IV)−O bonds between the Zr_6 node and carboxylate linkers result in excellent chemical and thermal stability properties for Zr-MOFs.[31] Through systematic investigations, we determined that greater accessibility to the Lewis acidic Zr_6 nodes (e.g., larger pore apertures, lower node connectivities, and smaller particle sizes) generally results in the faster catalytic hydrolysis of organophosphorus substrates,[32] and our team has recently demonstrated that Zr-MOF/textile composites are capable of hydrolyzing nerve agents under practical conditions using only water that is present as humidity.[33] As part of our continued efforts to improve the performance of organophosphorus hydrolysis catalysts, we extended our investigation to include other stable MOFs with Lewis acidic sites to complement the highly capable Zr- and Ce-based MOFs we studied previously.[27,34] Specifically, we drew inspiration from the carbonic anhydrase (CA) class of metalloenzymes.[35,36] In addition to CO_2 hydration, CAs are also capable of hydrolyzing esters and phosphonate esters with performance similar to that of other enzymes, such as esterase phosphatase.[37] Hydrolysis in CAs occurs at the Zn(II)−OH active sites (Figure 1e) in which the electronegative OH^- group acts as a nucleophile that attacks the partially electropositive central atom of the ester or phosphonate ester (i.e., carbonyl or phosphorus atom), forming an intermediate from which the C−O or P−O bond is subsequently cleaved.[38] However, the lack of thermal stability, long-term stability, and high cost of CAs limit their practical use. Therefore, we considered MOFs that contain nodes with accessible Zn(II)−OH groups coordinated to nitrogen-based ligands as potential CA mimics that may exhibit similar reactivity to these enzymes with improved thermal and chemical stability.

In this work, we investigate the Zn triazole-based MOF MFU-4l, which is constructed with 6-connected Zn_5 nodes and bis(1*H*-1,2,3-triazolo-[4,5-*b*],[4′,5′-*i*])dibenzo-[1,4]-dioxin (H_2-BTDD) linkers (Figure 1c).[39] Four of the Zn(II) ions are tetrahedrally coordinated by three linkers and one Cl^- anion, and one Zn(II) ion is octahedrally coordinated by six $BTDD^{2-}$ linkers. MFU-4l exhibits good chemical stability in basic aqueous solutions, and spectroscopic studies reveal that under these conditions the Cl^- ions coordinated to Zn(II) in the parent MFU-4l are rapidly replaced with OH^- groups, forming the Zn(II)−OH group that is reminiscent of the active sites found in CAs. Importantly, MFU-4l is an extremely effective catalyst for the hydrolysis of the nerve agent GD and the nerve agent simulant DMNP in basic aqueous solutions with half-lives of 3.3 and <1 min, respectively, which are among the best for MOF-based catalysts employed under similar conditions, thus paving the way toward a new class of organophosphorus nerve agent hydrolysis catalysts.

EXPERIMENTAL SECTION

MFU-4l was prepared through the solvothermal synthesis in dimethylformamide (DMF) at 140 °C for 18 h (see the Supporting Information for more details). Bulk phase purity of the activated materials was confirmed through powder X-ray diffraction (PXRD) analysis as the obtained experimental pattern is consistent with the simulated pattern (Figure 2a). Scanning electron microscope (SEM) images reveal a cubic morphology with particle sizes ranging from 300 to 800 nm, as expected from the cubic unit cell of MFU-4l (Figure S1). The Brunauer−Emmett−Teller (BET) area and pore volume are calculated to be 3430 $cm^2\ g^{-1}$ and 1.13 $cm^3\ g^{-1}$, respectively, which were obtained from N_2 isotherms collected at 77 K (Figure 2b).

https://dx.doi.org/10.1021/acs.chemmater.0c02373
Chem. Mater. XXXX, XXX, XXX−XXX

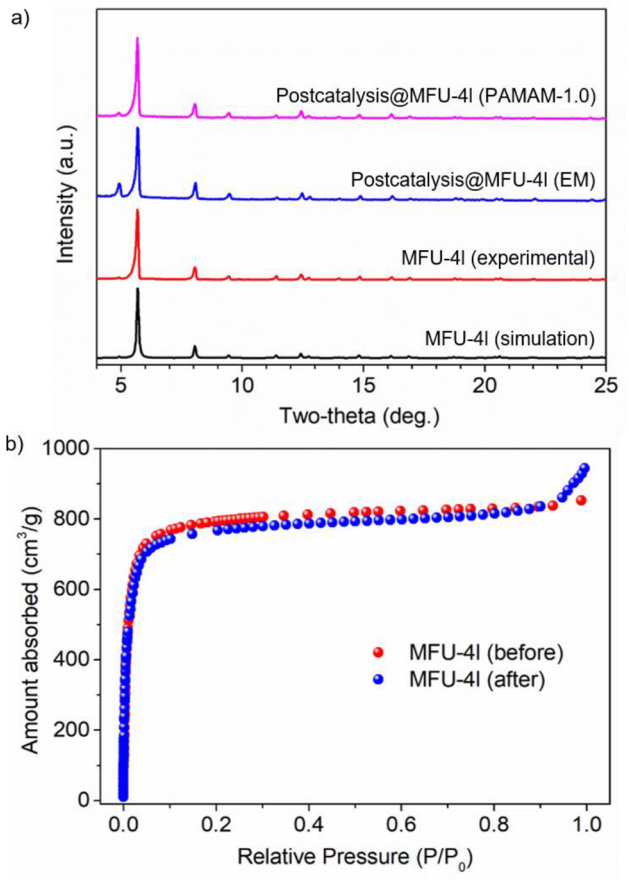

Figure 2. (a) PXRD patterns of MFU-4l (black is simulation and red is experimental) and postcatalysis samples of MFU-4l with either EM (blue) or PAMAM-1.0 (pink). (b) N_2 isotherms at 77 K for MFU-4l (red) and after soaking the MFU-4l in EM solution for 20 min (blue).

Hydrolysis of DMNP. Catalysis experiments were performed by *in situ* ^{31}P NMR spectroscopy at room temperature. 1.9 mg (6 mol %) of MFU-4l was added to 1.05 mL of EM solution (0.05 mL of EM (0.4 mmol), 0.9 mL of deionized water, and 0.1 mL of D_2O) in a 1.5 mL dram vial. The resulting mixture was stirred for 2 min to disperse the MOF powder. DMNP (4.0 μL, about 6.2 mg) was added to this suspension and swirled for 10 s. The reaction mixture was then transferred to an NMR tube, and the spectrum was immediately measured; the first data point was collected as fast as possible after the start of the reaction. The reaction progression was monitored by ^{31}P NMR spectroscopy via the formation of a dimethyl phosphate anion. For reactions with PAMAM-1.0, the amount of dendrimer was based on the same molar amount of nitrogen compared to EM (0.4 mmol). The volume of PAMAM-1.0 is 132 μL.

Hydrolysis of GD. 1.9 mg (6 mol %) of MFU-4l was added to 1.05 mL of EM or PAMAM-1.0 buffer in a 1.5 mL dram vial. The resulting mixture was stirred for 2 min to disperse the MOF powder. GD (4.4 μL, 25 μmol) was added to this suspension. The reaction progression was monitored by ^{31}P NMR spectroscopy via the formation of pinacolyl methylphosphonic acid (PMPA).

RESULTS AND DISCUSSION

After confirming the structural purity and permanent porosity of MFU-4l, we evaluated the catalytic activity of MFU-4l against the hydrolysis of the nerve agent simulant dimethyl (4-nitrophenyl)phosphate (DMNP, Figure 1a). We hypothesized that under catalytically relevant conditions in basic aqueous solutions, Cl^- ions would be replaced with OH^- groups *in situ* to form Zn(II)−OH sites, so catalytic reactions were conducted with MFU-4l powders without any chemical modification. Initial hydrolysis reactions were performed with 6 mol % catalyst loading in pH 10.5 solution at room temperature by using *N*-ethylmorpholine (EM) as the base (see the Supporting Information for more details), and ^{31}P NMR spectroscopy was used to monitor the reaction progress (Figure 3a). As the reaction proceeds, the peak around −4.4

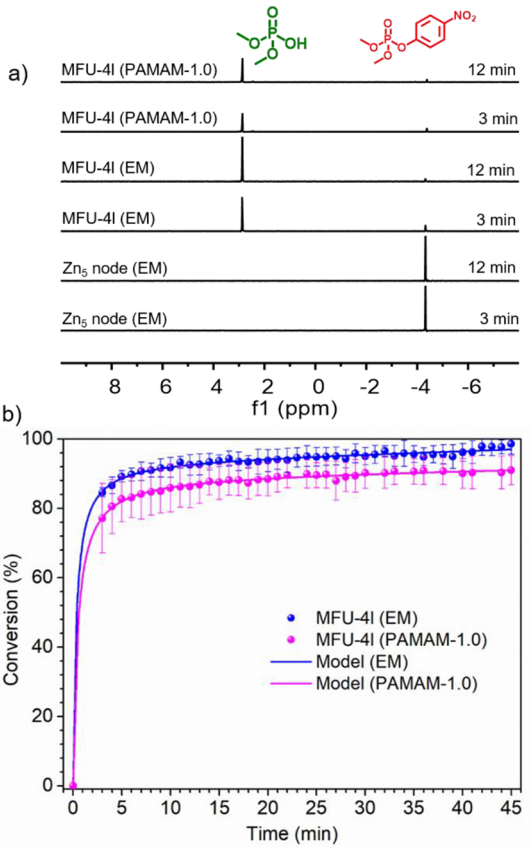

Figure 3. (a) ^{31}P NMR spectra obtained from the hydrolysis of DMNP (δ = −4.4 ppm) to the dimethoxy phosphate anion (δ = 2.8 ppm) with the Zr_5 node and MFU-4l with EM and PAMAM-1.0 as the base at different time points. (b) Kinetic profiles of DMNP hydrolysis with MFU-4l using 6 mol % catalyst loading in the presence of EM (blue) and PAMAM-1.0 (pink) as the base.

ppm that corresponds to DMNP disappears, and a new peak appears at 2.8 ppm, indicating the formation of the dimethyl phosphate anion;[32,41] the relative ratios obtained from integrating these two peaks are used to construct kinetic profiles (Figure 3b). When MFU-4l is employed as a catalyst under these conditions, more than 80% of DMNP is converted to the benign phosphate product in under 3 min, and a first-order kinetic equation was used to calculate the initial reaction rate constants and half-lives.[40] Notably, the calculated half-life ($t_{1/2}$) for hydrolysis of DMNP is <1 min, which is comparable to those of the some of the best Zr-MOF hydrolysis catalysts, MOF-808 and NU-901 ($t_{1/2}$ = <0.5 and 1 min, respectively, Table 1).[41,42] Additionally, decreasing the amount of MFU-4l to 3 mol % results in a $t_{1/2}$ of 1.8 min for DMNP hydrolysis (Figure S2), and the initial rate constant was calculated to be 0.24 ± 0.01 min^{-1} (Figure S3).

Recently, we studied the performance of Zr-MOF hydrolysis catalysts when the volatile EM was replaced with a less volatile

https://dx.doi.org/10.1021/acs.chemmater.0c02373
Chem. Mater. XXXX, XXX, XXX−XXX

Table 1. Comparison between the Performance of Selected MOF Catalysts for the Hydrolysis of DMNP and GD[a]

MOF	simulant, real agent	$t_{1/2}$ (min)	ref
MFU-4l	DMNP, GD	<1, 3.3	this work
MOF-808	DMNP	<0.5[b]	42
NU-1000-dehy	DMNP	1.5	32
NU-1000	DMNP, GD	15, 3	32
NU-901	DMNP	1	41
UiO-66	DMNP	45	43
UiO-66-NH_2	DMNP	1	44
NU-1600	DMNP	1	45
Spirof-MOF-b	DMNP	1.8	46

[a]General conditions: 6 mol % MOF loading, 0.4 M EM, pH 10−10.5, H_2O. [b]1.5 mol % catalyst.

base, which is an important consideration for the use of these catalysts in practical applications, such as in protective suits or in filters used in masks, and found that the use of dendritic and polymeric amine bases results in nearly identical peformance.[41] Among these bases, the PAMAM-1.0 dendrimer achieved the best performance with the Zr-MOF system. On the basis of these previous results, we decided to test the PAMAM-1.0 dendrimer in DMNP hydrolysis reactions with MFU-4l, finding that $t_{1/2}$ = <1 min and that the kinetic profile for this reaction is comparable to that of the reaction performed with EM (Figure 3b).

To investigate the stability of MFU-4l following catalytic reactions, MFU-4l was filtered from the postcatalysis reaction mixture and dried after washing with methanol. The PXRD pattern obtained for this sample is preserved, which confirms the structural integrity of MFU-4l (Figure 2a). As a further control, we prepared the complex $[Zn_5Cl_4(bnz)_6]$ (bnz = benzotriazole), and single-crystal X-ray diffraction studies indicate that this complex has similar Zn_5 nodes to those found in MFU-4l (Figure S5a). Unlike the porous framework in MFU-4l, the dense packing of $[Zn_5Cl_4(bnz)_6]$ did not reveal any accessible internal void space (Figure S5b). Both crystals and ground powders of $[Zn_5Cl_4(bnz)_6]$ were used for DMNP hydrolysis under the reaction conditions previously described, but no measurable reactivity toward the hydrolysis of DMNP was observed after 15 min (Figure 3a); around 20% conversion was observed 3 h later (Figure S7) which can be attributed to the Zn(II)−OH sites on the surface of crystals. These results suggest that MFU-4l acts as a heterogeneous catalyst and that the ditopic BTDD linker yields a highly porous network that provides sufficient distance between the Zn_5 active sites in MFU-4l to enable DMNP access, highlighting the importance of porosity in heterogeneous catalysis.

As previous studies indicate that Zn(II)−OH sites (pK_a = 9.0 ± 0.1) are the reactive sites for the hydrolysis of organophosphorus compounds,[47] the observed hydrolytic reactivity for MFU-4l suggests the Cl^- capping ligands on the parent MFU-4l are replaced with OH^- ligands under the basic reaction conditions. We investigated the influence of pH on the catalytic activity observed for MFU-4l, finding that the reactivity is comparable in pH 10.5 and 9.5 solutions, but a significant decrease in reactivity is observed when the pH of the solution is reduced to 8.5 (Figure S4). The difference in reactivity is much more pronounced at the initial time points of each reaction relative to when the reactions plateau, suggesting the rate of replacement of Cl^- ligands by OH^- ligands occurs much faster at pH 9.5 and above.

To investigate the kinetics of Cl^-/OH^- ligand exchange for this system, MFU-4l was soaked in aqueous solutions of EM at pH 10.5 for 5, 10, 15, and 20 min. Solids were filtered and washed with acetone three times, then dried at 100 °C under vacuum for 60 min, and finally characterized by using multiple techniques. First, diffuse reflectance infrared Fourier transform spectroscopy (DRIFTS) was employed to monitor the presence of hydroxyl anions. According to the DRIFTS spectra presented in Figure 4a,b, a new band appears at 3700 cm^{-1} in all samples treated in EM solution that was not initially present in the DRIFTS spectrum obtained for the parent MFU-4l, which is attributed to the hydroxyl stretches of Zn(II)−OH. The intensity of this peak does not change significantly with time, suggesting that near complete conversion from Cl^- to OH^- occurs within 5 min.

Next, X-ray photoelectron spectroscopy (XPS) was used to quantify the amount of Cl present in each sample. A broad peak around 198 eV is observed for the parent MFU-4l, which

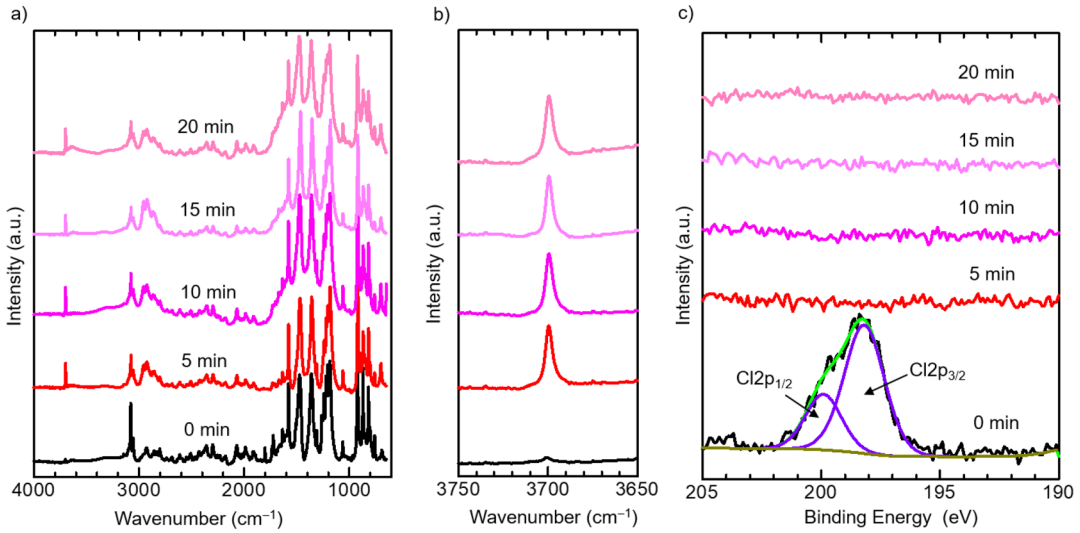

Figure 4. DRIFTS spectra (a, b) and XPS (c) core spectra for Cl 2p scans taken at different time points after treatment of MFU-4l in EM solutions at room temperature.

https://dx.doi.org/10.1021/acs.chemmater.0c02373
Chem. Mater. XXXX, XXX, XXX−XXX

corresponds to binding energy of 2p core electrons in Cl (Figure 4c). The peak could be separated into doublets ($2p_{3/2}$ and $2p_{1/2}$) by using a Gaussian−Lorentzian line fitting. After soaking the sample in EM solution for 5 min, no detectable peak beyond background noise is observed in the region, indicating that all Cl^- ions have been replaced with OH^- ions by this time point. Furthermore, EDX spectra obtained for MFU-4l show 4.8 wt % Cl, whereas the amount of Cl is found to be 0.4 wt % and below after soaking MFU-4l in EM for 5, 10, 15, and 20 min (Figure S8); the small amount of Cl observed in the EDX spectra is due to the background noise (Figures S9 and S10). Finally, the N_2 adsorption isotherm collected for a sample of MFU-4l soaked in EM solution for 20 min shows a BET area of 3350 $cm^2\ g^{-1}$, which is comparable to the BET area of 3430 $cm^2\ g^{-1}$ obtained for the parent MFU-4l (Figure 2b). SEM images reveal that the cubic morphology of MFU-4l is maintained even after soaking in EM solution (Figure S1). Overall, all spectroscopic studies indicate that upon soaking in EM solutions at pH 10.5 the Cl^- ligands are replaced with OH^- groups within 5 min, at which point most of the DMNP is consumed, suggesting that the Zn(II)−OH sites are the active sites for the hydrolysis of DMNP.

After determining that MFU-4l is capable of rapidly hydrolyzing DMNP in basic aqueous solutions, we decided to investigate the reactivity of MFU-4l toward the actual nerve agent soman, also known as GD. Hydrolysis reactions were conducted using 6 mol % MFU-4l as the catalyst and either EM or PAMAM-1.0 as the base, and progress of the reaction was monitored via ^{31}P NMR spectroscopy (Figure S11). As the reaction proceeds, two doublets around 31 and 37 ppm that correspond to GD decrease in intensity, and a singlet assigned to the nontoxic hydrolysis product, pinacolyl methylphosphonic acid (PMPA), appears at 25 ppm.[32,33] The hydrolytic reactivity of MFU-4l toward GD in solutions of EM and PAMAM-1.0 is comparable to that observed for DMNP hydrolysis, with calculated half-lives of 3.3 and 4.0 min, respectively (Figure 5), and the initial rate constant for GD

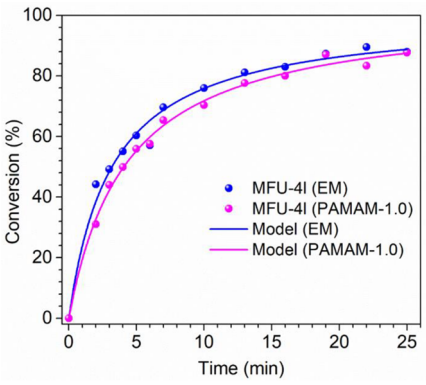

Figure 5. Hydrolysis profile of GD with MFU-4l using 6 mol % catalysts loading in the presence of EM (blue) and PAMAM-1.0 dendrimer (pink).

hydrolysis in EM solution was calculated to be 0.18 ± 0.03 min^{-1} (Figure S12). Overall, these data place MFU-4l among the most active heterogeneous GD hydrolysis catalysts reported to date under these conditions.[27]

CONCLUSION

We have demonstrated that MFU-4l, a Zn-triazole-based MOF, can catalyze the rapid hydrolysis of the organophosphorus nerve agent, GD, and its simulant, DMNP, with half-lives of 3.3 and <1 min, respectively. The combination of soft Lewis acidic Zn(II) and soft Lewis basic triazole-based building blocks of MFU-4l yields a heterogeneous catalyst that is stable under basic conditions. Spectroscopic studies reveal that the *in situ* ligand exchange from Cl^- to OH^- occurs within minutes to form the Zn(II)−OH species, which resemble the active site of the CA enzyme. Reactions performed under analogous conditions by using the nonporous, molecular Zn_5 cluster $[Zn_5Cl_4(bnz)_6]$ show negligible hydrolysis of DMNP, emphasizing the importance of organophosphorus substrate accessibility to the internal active sites in MFU-4l for efficient catalysis to occur. We anticipate that these results will pave the way toward the design of even more efficient Zn-azolate-based heterogeneous catalysts for the hydrolysis of organophosphorus nerve agents.

ASSOCIATED CONTENT

Supporting Information

The Supporting Information is available free of charge at https://pubs.acs.org/doi/10.1021/acs.chemmater.0c02373.

Instrumentation, syntheses of MFU-4l and $[Zn_5Cl_4(bnz)_6]$, hydrolysis procedure details, SEM image, crystal structure and crystallographic data for $[Zn_5Cl_4(bnz)_6]$, EDX, SEM-EDX mapping, XPS analysis, and NMR spectra (PDF)

Crystallographic data for $[Zn_5Cl_4(bnz)_6]$ (CIF)

AUTHOR INFORMATION

Corresponding Authors

Timur Islamoglu − *International Institute of Nanotechnology and Department of Chemistry, Northwestern University, Evanston, Illinois 60208, United States;* orcid.org/0000-0003-3688-9158; Email: timur.islamoglu@northwestern.edu

Omar K. Farha − *International Institute of Nanotechnology and Department of Chemistry and Department of Chemical & Biological Engineering, Northwestern University, Evanston, Illinois 60208, United States;* orcid.org/0000-0002-9904-9845; Email: o-farha@northwestern.edu

Authors

Mohammad Rasel Mian − *International Institute of Nanotechnology and Department of Chemistry, Northwestern University, Evanston, Illinois 60208, United States;* orcid.org/0000-0002-3034-8054

Unjila Afrin − *International Institute of Nanotechnology and Department of Chemistry, Northwestern University, Evanston, Illinois 60208, United States*

Subhadip Goswami − *International Institute of Nanotechnology and Department of Chemistry, Northwestern University, Evanston, Illinois 60208, United States;* orcid.org/0000-0002-8462-9054

Ran Cao − *International Institute of Nanotechnology and Department of Chemistry, Northwestern University, Evanston, Illinois 60208, United States*

Kent O. Kirlikovali − *International Institute of Nanotechnology and Department of Chemistry, Northwestern University, Evanston, Illinois 60208, United States;* orcid.org/0000-0001-8329-1015

https://dx.doi.org/10.1021/acs.chemmater.0c02373
Chem. Mater. XXXX, XXX, XXX−XXX

Morgan G. Hall − *CCDC Chemical Biological Center, Aberdeen Proving Ground, Maryland 21010, United States*
Gregory W. Peterson − *CCDC Chemical Biological Center, Aberdeen Proving Ground, Maryland 21010, United States;* orcid.org/0000-0003-3467-5295

Complete contact information is available at: https://pubs.acs.org/10.1021/acs.chemmater.0c02373

Author Contributions

M.R.M. and T.I. contributed equally to this work.

Notes

The authors declare no competing financial interest.

■ ACKNOWLEDGMENTS

The authors gratefully acknowledge support from the Defense Threat Reduction Agency (HDTRA1-18-1-0003). Use was made of the IMSERC X-ray facility at Northwestern University, which has received support from the Soft and Hybrid Nanotechnology Experimental (SHyNE) Resource (NSF ECCS-1542205), the State of Illinois, and the International Institute for Nanotechnology (IIN). This work made use of the EPIC facility of Northwestern University's NUANCE Center, which has received support from the Soft and Hybrid Nanotechnology Experimental (SHyNE) Resource (NSFECCS-1542205), the MRSEC program (NSF DMR-1720139) at the Materials Research Center, the International Institute for Nanotechnology (IIN), the Keck Foundation, and the State of Illinois through the IIN. K.O.K. gratefully acknowledges support from the IIN Postdoctoral Fellowship and the Northwestern University International Institute for Nanotechnology.

■ REFERENCES

(1) Organisation for the Prohibition of Chemical Weapons. "Addressing the Threat From Chemical Weapons Use". Ltamenah (Syrian Arab Repubic), 24, 25, and 30 March 2017 (https://www.opcw.org/sites/default/files/documents/2020/04/s-1867-2020%28e%29.pdf).
(2) Worek, F.; Wille, T.; Koller, M.; Thiermann, H. Toxicology of Organophosphorus Compounds in View of an Increasing Terrorist Threat. *Arch. Toxicol.* **2016**, *90*, 2131−2145.
(3) Enserink, M. U.N. Taps Special Labs to Investigate Syrian Attack. *Science* **2013**, *341*, 1050−1051.
(4) Eddleston, M.; Buckley, N. A; Eyer, P.; Dawson, A. H Management of Acute Organophosphorus Poisoning. *Lancet* **2008**, *371*, 597−607.
(5) Vanhooke, J. L.; Benning, M. M.; Raushel, F. M.; Holden, H. M. Three-Dimensional Structure of the Zinc-Containing Phosphotriesterase with the Bound Substrate Analog Diethyl 4-Methylbenzyl-phosphonate. *Biochemistry* **1996**, *35*, 6020−6025.
(6) Bigley, A. N.; Raushel, F. M. Catalytic Mechanisms for Phosphotriesterases. *Biochim. Biophys. Acta, Proteins Proteomics* **2013**, *1834*, 443−453.
(7) Wong, K.-Y.; Gao, J. The Reaction Mechanism of Paraoxon Hydrolysis by Phosphotriesterase from Combined QM/MMSimulations. *Biochemistry* **2007**, *46*, 13352−13369.
(8) Yang, Y. C.; Baker, J. A.; Ward, J. R. Decontamination of chemical warfare agents. *Chem. Rev.* **1992**, *92*, 1729−1743.
(9) Tsai, P.; Bigley, A.; Li, Y.; Ghanem, E.; Cadieux, C. L.; Kasten, S. A.; Reeves, T. E.; Cerasoli, D. M.; Raushel, F. M. Stereoselective Hydrolysis of Organophosphate Nerve Agent by the Bacterial Phosphotriesterase. *Biochemistry* **2010**, *49*, 7978−7987.
(10) Prokop, Z.; Oplustil, F.; DeFrank, J.; Damborsky, J. Enzymes Fight Chemical Weapons. *Biotechnol. J.* **2006**, *1*, 1370−1380.
(11) Ghanem, E.; Raushel, F. M. Detoxification of Organophosphate Nerve Agentsby Bacterial Phosphotriesterase. *Toxicol. Appl. Pharmacol.* **2005**, *207*, 459−470.
(12) Nath, I.; Chakraborty, J.; Verpoort, F. Metal Organic Frameworks Mimicking Natural Enzymes: A Structural and Functional Analogy. *Chem. Soc. Rev.* **2016**, *45*, 4127−4170.
(13) Wasson, M. C.; Buru, C. T.; Chen, Z.; Islamoglu, T.; Farha, O. K. Metal-Organic Frameworks: A Tunable Platform to Access Single-Site Heterogeneous Catalysts. *Appl. Catal., A* **2019**, *586*, 117214.
(14) Chen, Y.; Ma, S. Biomimetic Catalysis of Metal-Organic Frameworks. *Dalton Trans.* **2016**, *45*, 9744−9753.
(15) Baek, J.; Rungtaweevoranit, B.; Pei, X.; Park, M.; Fakra, S. C.; Liu, Y.-S.; Matheu, R.; Alshmimri, S. A.; Alshehri, S.; Trickett, C. A.; Somorjai, G. A.; Yaghi, O. M. Bioinspired Metal-Organic Framework Catalysts for Selective Methane Oxidation to Methanol. *J. Am. Chem. Soc.* **2018**, *140*, 18208−18216.
(16) Zhao, M.; Ou, S.; Wu, C. Porous Metal-Organic Frameworks for Heterogeneous Biomimetic Catalysis. *Acc. Chem. Res.* **2014**, *47*, 1199−1207.
(17) Xu, M.; Feng, L.; Yan, L.; Meng, S.; Yuan, S.; He, M.; Liang, H.; Chen, X.; Wei, H.; Gu, Z.; Zhou, H. Discovery of Precise Ph-Controlled Biomimetic Catalysts: Defective Zirconium Metal-Organic Frameworks as Alkaline Phosphatase Mimics. *Nanoscale* **2019**, *11*, 11270−11278.
(18) Gu, Z.; Park, J.; Raiff, A.; Wei, Z.; Zhou, H. Metal-Organic Frameworks as Biomimetic Catalysts. *ChemCatChem* **2014**, *6*, 67−75.
(19) Islamoglu, T.; Chen, Z.; Wasson, M. C.; Buru, C. T.; Kirlikovali, K. O.; Afrin, U.; Mian, M. R.; Farha, O. K. Metal-Organic Frame Works against Toxic Chemicals. *Chem. Rev.* **2020**, DOI: 10.1021/acs.chemrev.9b00828.
(20) Yaghi, O.; O'Keeffe, M.; Ockwig, N.; Chae, H. K.; Eddaoudi, M.; Kim, J. Reticular Synthesis and the Design of New Materials. *Nature* **2003**, *423*, 705−714.
(21) Furukawa, H.; Cordova, K. E.; O'Keeffe, M.; Yaghi, O. M. The Chemistry and Applications of Metal-Organic Frameworks. *Science* **2013**, *341*, 1230444.
(22) Li, J.-R.; Kuppler, R. J.; Zhou, H.-C. Selective Gas Adsorption and Separation in Metal-Organic Frameworks. *Chem. Soc. Rev.* **2009**, *38*, 1477−1504.
(23) Duan, J.; Jin, W.; Kitagawa, S. Water-Resistant Porous Coordination Polymers for Gas Separation. *Coord. Chem. Rev.* **2017**, *332*, 48−74.
(24) Wright, A. M.; Wu, Z.; Zhang, G.; Mancuso, J. L.; Comito, R. J.; Day, R. W.; Hendon, C. H.; Miller, J. T.; Dincă, M. A Structural Mimic of Carbonic Anhydrase in a Metal-Organic Framework. *Chem.* **2018**, *4*, 2894−2901.
(25) Li, B.; Wen, H.; Wang, H.; Wu, H.; Tyagi, M.; Yildirim, T.; Zhou, W.; Chen, B. A Porous Metal-Organic Framework with Dynamic Pyrimidine Groups Exhibiting Record High Methane Storage Working Capacity. *J. Am. Chem. Soc.* **2014**, *136*, 6207−6210.
(26) DeCoste, J. B.; Peterson, G. W. Metal-Organic Frameworks for Air Purification of Toxic Chemicals. *Chem. Rev.* **2014**, *114*, 5695−5727.
(27) Kirlikovali, K. O.; Chen, Z.; Islamoglu, T.; Hupp, J. T.; Farha, O. K. Zirconium-Based Metal-Organic Frameworks for the Catalytic Hydrolysis of Organophosphorus Nerve Agents. *ACS Appl. Mater. Interfaces* **2020**, *12*, 14702−14720.
(28) de Koning, M. C.; van Grol, M.; Breijaert, T. Degradation of Paraoxon and the Chemical Warfare Agents VX, Tabun, and Soman by the Metal-Organic Frameworks UiO-66-NH_2, MOF-808, NU-1000, and PCN-777. *Inorg. Chem.* **2017**, *56*, 11804−11809.
(29) Palomba, J. M.; Credille, C. V.; Kalaj, M.; DeCoste, J. B.; Peterson, G. W.; Tovar, T. M.; Cohen, S. M. High-Throughput Screening of Solid-State Catalysts for Nerve Agent Degradation. *Chem. Commun.* **2018**, *54*, 5768−5771.
(30) Peterson, G. W.; Lu, A. X.; Hall, M. G.; Browe, M. A.; Tovar, T.; Epps, T. H. MOFwich: Sandwiched Metal-Organic Framework-Containing Mixed Matrix Composites for Chemical Warfare Agent Removal. *ACS Appl. Mater. Interfaces* **2018**, *10*, 6820−6824.

(31) Howarth, A. J.; Liu, Y.; Li, P.; Li, Z.; Wang, T. C.; Hupp, J. T.; Farha, O. K. Chemical, Thermal and Mechanical Stabilities of Metal-Organic Frameworks. *Nat. Rev. Mater.* **2016**, *1*, 15018.
(32) Mondloch, J. E.; Katz, M. J.; Isley, W. C., III; Ghosh, P.; Liao, P.; Bury, W.; Wagner, G. W.; Hall, M. G.; DeCoste, J. B.; Peterson, G. W.; Snurr, R. Q.; Cramer, C. J.; Hupp, J. T.; Farha, O. K. Destruction of Chemical Warfare Agents Using Metal-Organic Frameworks. *Nat. Mater.* **2015**, *14*, 512−516.
(33) Chen, Z.; Ma, K.; Mahle, J. J.; Wang, H.; Syed, Z. H.; Atilgan, A.; Chen, Y.; Xin, J. H.; Islamoglu, T.; Peterson, G. W.; Farha, O. K. Integration of Metal-Organic Frameworks on Protective Layers for Destruction of Nerve Agents under Relevant Conditions. *J. Am. Chem. Soc.* **2019**, *141*, 20016−20021.
(34) Islamoglu, T.; Atilgan, A.; Moon, S.-Y.; Peterson, G. W.; DeCoste, J. B.; Hall, M.; Hupp, J. T.; Farha, O. K. Cerium(IV) vs Zirconium(IV) Based Metal-Organic Frameworks for Detoxification of a Nerve Agent. *Chem. Mater.* **2017**, *29*, 2672−2675.
(35) Supuran, C. T. Carbonic Anhydrases as Drug Targets-General Presentation. In *Drug Design of Zinc-Enzyme Inhibitors: Functional, Structural, and Disease Applications*; Supuran, C. T., Winum, J. Y., Eds.; Wiley: Hoboken, NJ, 2009; pp 15−38.
(36) Supuran, C. T. Carbonic Anhydrases: Novel Therapeutic Applications for Inhibitors and Activators. *Nat. Rev. Drug Discovery* **2008**, *7*, 168.
(37) Innocenti, A.; Supuran, C. T. Paraoxon, 4-Nitrophenyl Phosphate and Acetate Are Substrates Of nn but Not Of uuuuuu and nnCarbonic Anhydrases. *Bioorg. Med. Chem. Lett.* **2010**, *20*, 6208−6212.
(38) Makam, P.; Yamijala, S.; Tao, K.; Shimon, L. J. W.; Eisenberg, D. S.; Sawaya, M. R.; Wong, B. M.; Gazit, E. Non-Proteinaceous Hydrolase Composed of A Phenylalanine Metallo-Supramolecular Amyloid-Like Structure. *Nat. Catal.* **2019**, *2*, 977−985.
(39) Biswas, S.; Grzywa, M.; Nayek, H. P.; Dehnen, S.; Senkovska, I.; Kaskel, S.; Volkmer, D. A Cubic Coordination Framework Constructed from Benzobistriazolate Ligands and Zinc Ions Having Selective Gas Sorption Properties. *Dalton Trans.* **2009**, 6487−6495.
(40) Ploskonka, A. M.; DeCoste, J. B. Insight into Organophosphate Chemical Warfare Agent Simulant Hydroylsis in Metal-OrganicFrameworks. *J. Hazard. Mater.* **2019**, *375*, 191−197.
(41) Chen, Z.; Islamoglu, T.; Farha, O. K. Toward Base Heterogenization: A Zirconium Metal-Organic Framework/Dendrimeror Polymer Mixture for Rapid Hydrolysis of a Nerve-Agent Simulant. *ACS Appl. Nano Mater.* **2019**, *2*, 1005−1008.
(42) Moon, S.-Y.; Liu, Y.; Hupp, J. T.; Farha, O. K. Instantaneous Hydrolysis of Nerve-Agent Simulants with a Six-Connected Zirconium-Based Metal-Organic Framework. *Angew. Chem., Int. Ed.* **2015**, *54*, 6795−6799.
(43) Katz, M. J.; Mondloch, J. E.; Totten, R. K.; Park, J. K.; Nguyen, S. T.; Farha, O. K.; Hupp, J. T. Simple and Compelling Biomimetic Metal-Organic Framework Catalyst for the Degradation of Nerve Agent Simulants. *Angew. Chem.* **2014**, *126*, 507−511.
(44) Katz, M. J.; Moon, S.-Y.; Mondloch, J. E.; Beyzavi, M. H.; Stephenson, C. J.; Hupp, J. T.; Farha, O. K. Exploiting Parameter Space in MOFs: a 20-fold Enhancement of Phosphate-Ester Hydrolysis with UiO-66-NH_2. *Chem. Sci.* **2015**, *6*, 2286−2291.
(45) Chen, Z.; Li, P.; Wang, X.; Otake, K.-i.; Zhang, X.; Robison, L.; Atilgan, A.; Islamoglu, T.; Hall, M. G.; Peterson, G. W.; Stoddart, J. F.; Farha, O. K. Ligand-Directed Reticular Synthesis of Catalytically Active Missing Zirconium-Based Metal-Organic Frameworks. *J. Am. Chem. Soc.* **2019**, *141*, 12229−12235.
(46) Park, H. J.; Jang, J. K.; Kim, S.-Y.; Ha, J.-W.; Moon, D.; Kang, I.-N.; Bae, Y.-S.; Kim, S.; Hwang, D.-H. Synthesis of a Zr-Based Metal-Organic Framework with Spirobifluorenetetrabenzoic Acid for the Effective Removal of Nerve Agent Simulants. *Inorg. Chem.* **2017**, *56*, 12098−12101.
(47) Zastrow, M. L.; Pecoraro, V. L. Designing Hydrolytic Zinc Metalloenzymes. *Biochemistry* **2014**, *53*, 957−978.

https://dx.doi.org/10.1021/acs.chemmater.0c02373
Chem. Mater. XXXX, XXX, XXX−XXX